HHS Public Access

Author manuscript

Nat Methods. Author manuscript; available in PMC 2016 November 02.

Published in final edited form as:

Nat Methods. 2016 June ; 13(6): 497–500. doi:10.1038/nmeth.3852.

An unbiased metric of antiproliferative drug effect *in vitro*

Leonard A. Harris[1,2,5], **Peter L. Frick**[1,2,5], **Shawn P. Garbett**[1,2], **Keisha N. Hardeman**[1,2], **B. Bishal Paudel**[1,2], **Carlos F. Lopez**[1,3,4], **Vito Quaranta**[1,2], and **Darren R. Tyson**[1,2]

[1]Department of Cancer Biology, Vanderbilt University School of Medicine, Nashville, Tennessee, USA

[2]Center for Cancer Systems Biology at Vanderbilt, Vanderbilt University School of Medicine, Nashville, Tennessee, USA

[3]Department of Biomedical Informatics, Vanderbilt University School of Medicine, Nashville, Tennessee, USA

[4]Department of Biomedical Engineering, Vanderbilt University, Nashville, Tennessee, USA

Abstract

In vitro cell proliferation assays are widely used in pharmacology, molecular biology, and drug discovery. Using theoretical modeling and experimentation, we show that current antiproliferative drug effect metrics suffer from time-dependent bias, leading to inaccurate assessments of parameters such as drug potency and efficacy. We propose the drug-induced proliferation (DIP) rate, the slope of the line on a plot of cell population doublings versus time, as an alternative, time-independent metric.

MAIN TEXT

Evaluating antiproliferative drug activity on cells *in vitro* is a widespread practice in basic biomedical research[1–3] and drug discovery[4–6]. Typically, quantitative assessment relies on constructing dose–response curves[7] (Supplementary Note and Supplementary Fig. 1). Briefly, a drug is added over a range of concentrations and the effect on the cell population is quantified with a metric of choice[8]. The *de facto* standard metric is the number of viable cells 72 h after drug addition[4,6,8,9]. Being a single-time-point measurement, we refer to this as a "static" drug effect metric. The data is then fit to the Hill equation[10], a four-parameter log-logistic function, to produce a sigmoidal dose–response curve that summarizes the relationship between drug effect and concentration. Parameters extracted from these curves include the maximum effect (E_{max}), the half-maximal effective concentration (EC_{50}), the half-maximal inhibitory concentration (IC_{50}), area under the curve (AUC), and activity area

Correspondence should be addressed to: Darren R. Tyson (darren.tyson@vanderbilt.edu).

[5]These authors contributed equally to this work.

AUTHOR CONTRIBUTIONS

DRT, LAH, PLF, SPG conceived and designed the study; DRT, LAH, SPG built the mathematical models and performed simulations; BBP, KNH, PLF acquired experimental data; DRT, LAH, PLF, SPG analyzed and interpreted the experimental data; CFL, DRT, LAH, PLF, SPG, VQ wrote, reviewed, and/or revised the manuscript; CFL, DRT, VQ supervised the study.

(AA)[4,6,8,9] (Supplementary Fig. 1 and Supplementary Table 1). These are useful for quantitatively comparing various aspects of drug activity across drugs and cell lines.

We contend that dose–response curves constructed using current standard metrics of drug effect can result in erroneous and misleading values of drug-activity parameters, skewing data interpretation. This is because they suffer from time-dependent bias, i.e., the metric value varies with the time point chosen for experimental measurement. We identify two specific sources of time-dependent bias: (i) exponential growth, and (ii) delays in drug effect stabilization. The former can lead to erroneous conclusions, e.g., that a drug is increasing in effectiveness over time, while the latter requires shifting the window of evaluation to only include data points after stabilization has been achieved (Supplementary Fig. 2).

To overcome this problem of bias, we propose as an alternative drug effect metric the drug-induced proliferation (DIP) rate[11,12], defined as the steady-state rate of proliferation of a cell population in the presence of a given concentration of drug. Previously, with related approaches, we quantified clonal fitness[12] and heterogeneous single-cell fates[11] within cell populations responding to perturbations. Here, we show that DIP rate is an ideal metric of antiproliferative drug effect because it naturally avoids the bias afflicting traditional metrics, it is easily quantified as the slope of the line on a plot of cell-population doublings versus time (Supplementary Fig. 2), and it is interpretable biologically as the rate of regression or expansion of a cell population.

To theoretically illustrate the consequences of time-dependent bias in standard drug effect metrics, we constructed a simple mathematical model of cell proliferation that exhibits the salient features of cultured cell dynamics in response to drug (Online Methods, Supplementary Note, Supplementary Fig. 3, and Supplementary Table 2). The model assumes that cells experience two fates, division and death, and that the drug modulates the difference between the rates of these two processes, i.e., the net rate of proliferation. Drug action may occur immediately or gradually over time, depending on the chosen parameter values. In all cases, a stable DIP rate is eventually achieved, and when calculated over a range of drug concentrations a sigmoidal dose–response relationship emerges (Supplementary Note and Supplementary Fig. 3).

We model three scenarios: treatment of a fast-proliferating cell line with a fast-acting drug (Fig. 1a), a slow-proliferating cell line with a fast-acting drug (Fig. 1b), and a fast-proliferating cell line with a delayed-action drug (Fig. 1c). In each case, we generate simulated growth curves in the presence of increasing drug concentrations (Fig. 1, columns 1 and 2) and from these produce static dose–response curves by taking cell counts at single time points between 12h and 120h (Fig. 1, column 3). As expected, in each scenario the shape of the dose–response curve varies depending on the time of measurement. Consequently, parameter values extracted from these curves (EC_{50} and AA) also vary (Fig. 1, columns 4 and 5). Similar results are obtained for an alternative drug effect metric proposed by the U.S. National Cancer Institute's Developmental Therapeutics Program[13] (Supplementary Note and Supplementary Fig. 4). In contrast, DIP rate, being the slope of a line, is independent of measurement time. Using it as the drug effect metric gives a single

dose–response curve (Fig. 1, columns 3 and 6) and single values of the extracted drug-activity parameters (Fig. 1, columns 4 and 5).

As a first confirmation of our theoretical findings, we subjected triple-negative breast cancer cells (MDA-MB-231) to the metabolic inhibitors rotenone (Fig. 2a) and phenformin (Fig. 2b). Using fluorescence microscopy time-lapse imaging[11,12,14] (Online Methods), we quantified changes in cell number over time for a range of drug concentrations[18,19]. For both drugs, we observe a rapid stabilization of the drug effect (<24h delay) and stable exponential proliferation thereafter, reminiscent of the growth dynamics of the theoretical cell lines treated with fast-acting drugs (Fig. 1a,b). We generated dose–response curves from these data using the standard static effect metric and DIP rate for various drug exposure times. Consistent with our theoretical results, the shape of the static-based dose–response curve strongly depends on the time point at which cell counts are taken, an illustration of time-dependent bias. The DIP rate, on the other hand, is free of time-dependent bias and produces a single dose–response curve in both cases.

These DIP rate-based dose–response curves produce interesting insights (Fig. 2a,b). For example, they indicate that while rotenone is much more potent than phenformin ($EC_{50} \approx$ 8.5 nM versus 25 μM), phenformin is more effective ($E_{max}/E_0 \approx -0.1$ versus 0.1). The ordering of potencies (rotenone $\gg$ phenformin) could have been garnered from the static dose–response curves, but not the ordering of efficacies, i.e., the static drug effect metric obscures the crucial fact that at saturating concentrations phenformin is cytotoxic (causes cell population regression) while rotenone is partially cytostatic (cell populations continue to expand slowly). This information is obviously critical to studies assessing drug mechanism of action. This example illustrates the perils of biased drug effect metrics and the ability of DIP rate to produce reliable dose-response curves from which accurate quantitative and qualitative assessments of antiproliferative drug activity can be made.

To illustrate the confounding effects that a delay in the stabilization of the drug effect can have, we examined single-cell derived clones of the lung cancer cell line PC9, which is known to be hypersensitive to erlotinib[15], an epidermal growth factor receptor (EGFR) kinase inhibitor. Consistent with our previous report[11], three drug-sensitive PC9-derived clones (DS3, DS4, DS5) each respond to 3 μM erlotinib with nonlinear growth dynamics over the first 48–72h, followed by stable exponential proliferation thereafter (Fig. 2c). These dynamics are reminiscent of those for the theoretical fast-proliferating cell line with a delayed-action drug (Fig. 1c). Due to the delay in drug action, all three clones have nearly identical population sizes 72h after drug addition for all concentrations considered. The static 72h metric thus produces essentially identical dose–response curves for all clones (Supplementary Fig. 5). In contrast, dose–response curves based on DIP rate make a clear distinction between the clones in terms of their long-term response to drug, i.e., erlotinib is cytotoxic (negative DIP rate) for two of the clones but partially cytostatic (positive DIP rate) for the other (Fig. 2c).

We then investigated the effects of erlotinib and lapatinib (a dual EGFR/human EGFR 2 (HER2) kinase inhibitor) on HER2-positive breast cancer cells (HCC1954; delay ~48h; Fig. 2d). In each case, DIP rate-based dose–response curves produce EC_{50} values more than five-

fold larger than their static counterparts, i.e., by the static drug effect metric the drugs appear significantly more potent than they actually are. Taken together with the PC9 results (Fig. 2c), these data illustrate the importance of accounting for delays in drug action when assessing antiproliferative drug activity and further emphasize the ability of the DIP rate metric to produce accurate drug-activity parameters and qualitative conclusions about drug-response dynamics.

Within the last several years, a number of studies have been published reporting drug responses for hundreds of cell lines derived from various cancer types[4,6,9,16,17] and organ sites[8,18,19]. Raw data are available for the responses of over 1000 cancer cell lines to a panel of 24 drugs in the Cancer Cell Line Encyclopedia (CCLE)[6] and for over 1200 cell lines treated with 140 drugs in the Genomics of Drug Sensitivity in Cancer (GDSC) project[9]. These data are largely based on static measurements of cell number after 72h of drug exposure, a metric that we have shown here contains time-dependent bias.

To investigate bias in these datasets, we treated four $BRAF^{V600E \text{ or } D}$-expressing melanoma cell lines with various concentrations of the BRAF-targeted agent PLX4720, an analog of vemurafenib. We produced experimental growth curves (Fig. 3a), static- and DIP rate-based dose–response curves (Fig. 3b), and extracted IC_{50} values for each cell line and compared these to IC_{50} values obtained from the CCLE and GDSC data sets (Fig. 3c). In all cases, our IC_{50} values correspond closely to the value from at least one of the public data sets. While in three cases the static- and DIP rate-based IC_{50} values correspond within an order of magnitude, in one case (A375) they differ by nearly two orders of magnitude. This discrepancy can be traced to a period of complex, non-linear dynamics (brief regression followed by rebound) observed for this cell line between 24h and 72h post-drug addition (Fig. 3a). This result is particularly intriguing because it shows that, based on DIP rate, this cell line is not much different in terms of drug sensitivity than the other three. Using the biased static drug effect metric, however, one would be led to the incorrect conclusion that it is significantly more sensitive. It is very likely that cases like this abound within these and other similar data sets[16,17] and illustrates the critical need for new antiproliferative drug effect metrics.

Current protocols for cell proliferation assays are based on informal ‘rules of thumb’, for example, counting cells after 72 h of treatment to ameliorate the impact of complex dynamics and delays in drug response. However, these de facto standards have no theoretical basis and, as demonstrated here, they suffer from time-dependent bias that leads to erroneous conclusions. In light of the widespread applications of cell proliferation assays in oncology, pharmacology, and basic biomedical science[20] (for example, to assess activity of cytokines, cell surface receptors, altered signaling pathways, gene overexpression and silencing, or cell metabolic adaptation to varied microenvironmental conditions), it is imperative that the quality of the metric for antiproliferative assays be improved. Toward this end, we have proposed DIP rate as a viable, unbiased alternative antiproliferative drug effect metric. DIP rate overcomes time-dependent bias by log-scaling cell count measurements to account for exponential proliferation and by shifting the time window of evaluation to accommodate lag in the action of a drug, changes that do not substantially alter experimental design (Supplementary Note and Supplementary Figs. 6–9). Moreover, DIP rate is an

intuitive, biologically interpretable metric with a sound basis in theoretical population dynamics, and it faithfully captures, within a single value, the long-term effect of a drug on a cell population.

ONLINE METHODS

Dose–response curve fitting

All drug-response data (theoretical and experimental) were fit with a four-parameter log-logistic function (Supplementary Note) using nonlinear least-squares regression[21] within the R statistical programming environment (http://R-project.org). Fitting was performed using the drm function of the drc R library[22]. Ninety-five percent confidence intervals for each parameter were obtained using the delta method assuming asymptotic variance[21], as implemented within the confint function of the stats R library. EC_{50} is a fit parameter of the model. IC_{50} is the concentration at which $E_{\text{drug}} = E_0/2$ (Supplementary Fig. 1 and Supplementary Table 1), independent of the value of E_{max}, and is obtained using the ED function of the drc library. Activity area (AA; Supplementary Fig. 1) is calculated as

$$\text{AA} = -\sum_{i=1}^{N} (E_{drug,i}/E_0 - 1)/N \quad (1)$$

where $E_{\text{drug,i}}$ is the value of the effect metric at the i-th drug concentration and N is the total number of concentrations considered.

A simple two-state model of drug action on an exponentially proliferating cell population

We assume that cells can exist in two states, a “no-drug” and a “drug-saturated” state, and that cells in each state can experience two fates, division and death, with kinetic rate constants that are characteristic of the state, i.e., reflecting the effect of the drug (visual representation of the model is provided in Supplementary Fig. 3a). In the presence of drug, cells can transition from the no-drug to the drug-saturated state at a rate proportional to the concentration of drug. Reverse transitions occur at a rate independent of drug. If *Cell* is the number of cells in the no-drug state and *Cell** is the number of cells in the drug-saturated state, then the temporal dynamics of the drug-treated cell population is described by the following pair of coupled ordinary differential equations,

$$\frac{dCell}{dt} = (k_{div} - k_{death} - k_{on} Drug) \cdot Cell + k_{off} \cdot Cell^* \quad (2)$$

$$\frac{dCell^*}{dt} = (k_{div^*} - k_{death^*} - k_{off}) \cdot Cell^* + k_{on} \cdot Drug \cdot Cell \quad (3)$$

where k_{div} (k_{div}*) and k_{death} (k_{death}*) are the rate constants for cellular division and death, respectively, in the no-drug (drug-saturated) state, *Drug* is the drug concentration, k_{on} is the rate constant for the transition from the no-drug to the drug-saturated state, and k_{off} is the rate constant for the reverse transition.

At a given drug concentration (assumed to be constant, i.e., drug is neither consumed, removed, nor degraded), a population of cells will eventually reach a dynamic equilibrium in terms of the number of cells in each state. The effective DIP rate of a cell population is then the weighted average of the net proliferation rates (i.e., the difference between the division and death rate constants) of the two individual states (Supplementary Fig. 3b). With increasing drug concentration, the equilibrium shifts increasingly towards the drug-saturated state, asymptotically approaching 100% occupancy. The result is a sigmoidal dose–response relationship between DIP rate and drug concentration (Supplementary Fig. 3c,d). If the values of the rate constants governing the interconversion between the no-drug and drug-saturated state (k_{on} and k_{off}) are "large" (effectively infinite), then the dynamic equilibrium between states is achieved immediately upon drug addition. This is known as the partial equilibrium assumption (PEA)[23,24]. Mathematically, the PEA asserts that

$$k_{on} \cdot Drug \cdot Cell = k_{off} \cdot Cell^* \quad (4)$$

Under this assumption, an analytical solution for the total number of cells, $Cell_T = Cell + Cell^*$, can be obtained as a function of time,

$$\ln\frac{Cell_T(t)}{Cell_T(0)} = \frac{\frac{k_{off}}{k_{on}}(k_{div} - k_{death}) + Drug(k^*_{div} - k^*_{death})}{\frac{k_{off}}{k_{on}} + Drug} \cdot t \quad (5)$$

where $Cell_T(0)$ is the initial number of cells. All theoretical results shown in Figure 1a,b were obtained using equation (5). For the results in Figure 1c and Supplementary Figure 4, numerical integration of equations (2) and (3) was necessary since the values of k_{on} and k_{off} were set such that the PEA does not hold (Supplementary Table 2), i.e., there is a delay in the stabilization of the drug effect. Numerical integration was performed in R using the deSolve package[25]. For further details of the model, see Supplementary Note; for all parameter values used in this work, see Supplementary Table 2.

Cell lines

The PC9 cell line was originally obtained from William Pao (Vanderbilt University). WM115 cells were from Meenhard Herlyn (Wistar Institute). All other cell lines were obtained from the American Type Culture Collection (www.atcc.org). All cell lines are regularly tested for mycoplasma using a PCR-based method (MycoAlert, Lonza, Allendale, NJ) and any positive cultures are immediately discarded. Cell line authentication is provided by ATCC. Authenticity of PC9 and WM115 have not been verified.

Time-lapse fluorescence microscopic imaging

Time-lapse fluorescence microscopy of cells expressing histone H2B conjugated to monomeric red fluorescent protein (H2BmRFP) to facilitate automated image analysis for identifying and quantifying individual nuclei was performed as previously described[11,12,14]. Briefly, cells are engineered to express H2BmRFP using recombinant, replication-incompetent lentiviral particles and flow sorted for the highest 20% intensity. Cells are seeded at ~2,500 cells per well in 96-well imaging microtiter plates (BD Biosciences) and fluorescent nuclei are imaged using a BD Pathway 855 with a 20× objective in 3×3 montaged images per well at ~15 min intervals for 5 days. Alternatively, fluorescent cell nuclei are imaged twice daily using a Synentec Cellavista High End with a 20× objective and tiling of nine images. DIP rate-based dose–response curves shown in Figure 2c were generated from a single experiment performed at the Vanderbilt High-Throughput Screening Core on a Molecular Devices ImageXpress using similar imaging parameters. The experiment had two technical replicates per condition and images were obtained at 0, 24, 48, 52, 56, 60, 64, 68, 72, 76, 80, 84, 88, 92, 96,100,104,108, and 112 hours after addition of erlotinib at each of eight different concentrations or dimethyl sulfoxide (DMSO) control.

Other statistical considerations and code availability

Estimates of DIP rate are determined within an experiment using the sum of cells across all technical replicates at a given time point and obtaining the slope of a linear model of log2(cell number) ~ time for time points greater than the observed delay. Minimum delay time is estimated by visual inspection of log-growth curves for the time at which they become approximately linear (for an automated method of estimating the stabilization time point, see Supplementary Note and Supplementary Figs. 6 and 7). All data analysis was performed in R (version 3.2.1) and all raw data and R analysis code is freely available at github.com/QuLab-VU/DIP_rate_NatMeth2016.

Publicly available data sets

Drug-response data were obtained from the Genomics of Drug Sensitivity in Cancer (GDSC) project[4,9] website at ftp://ftp.sanger.ac.uk/pub/project/cancerrxgene/releases/release-5.0/gdsc_drug_sensitivity_raw_data_w5.zip and from the Cancer Cell Line Encyclopedia (CCLE)[6] website at http://www.broadinstitute.org/ccle/ in the data file CCLE_NP24.2009_Drug_data_2015.02.24.csv (user login required).

Supplementary Material

Refer to Web version on PubMed Central for supplementary material.

Acknowledgments

We are grateful to R. Feroze, J. Hao, K. Jameson, and C. Peng for support in experimental data acquisition; to J. Guinney, T. de Paulis, and J.R. Faeder for critical reviews of the manuscript; to W. Pao (Vanderbilt University, Nashville, Tennessee) for providing the PC9 cell line; and to M. Herlyn (Wistar Institute, Philadelphia, Pennsylvania) for providing the WM115 cell line. This work was supported by Uniting Against Lung Cancer 13020513 (D.R.T.), Vanderbilt Biomedical Informatics Training Program NLM 5T15-LM007450-14 (L.A.H.), and the National Cancer Institute U54-CA113007 (V.Q.), U01-CA174706 (V.Q.), and R01-CA186193 (V.Q.), and partially supported by the National Cancer Institute (P50-CA098131) and the National Center for Advancing Translational Sciences (UL1-TR000445-06). This work was also supported by the National Science Foundation

(grant MCB-1411482 to C.F.L.) and the VICC (Young Ambassador Award to C.F.L.). Its contents are solely the responsibility of the authors and do not necessarily represent official views of the National Cancer Institute, the National Center for Advancing Translational Sciences, or the National Institutes of Health.

REFERENCES FOR MAIN TEXT

1. Zuber J, et al. Toolkit for evaluating genes required for proliferation and survival using tetracycline-regulated RNAi. Nat Biotechnol. 2011; 29:79–83. [PubMed: 21131983]
2. Berns K, et al. A large-scale RNAi screen in human cells identifies new components of the p53 pathway. Nature. 2004; 428:431–437. [PubMed: 15042092]
3. Bonnans C, Chou J, Werb Z. Remodelling the extracellular matrix in development and disease. Nat Rev Mol Cell Biol. 2014; 15:786–801. [PubMed: 25415508]
4. Garnett MJ, et al. Systematic identification of genomic markers of drug sensitivity in cancer cells. Nature. 2012; 483:570–575. [PubMed: 22460902]
5. Wang L, McLeod HL, Weinshilboum RM. Genomics and drug response. N Engl J Med. 2011; 364:1144–1153. [PubMed: 21428770]
6. Barretina J, et al. The Cancer Cell Line Encyclopedia enables predictive modelling of anticancer drug sensitivity. Nature. 2012; 483:603–607. [PubMed: 22460905]
7. Stephenson RP. A modification of receptor theory. Br J Pharmacol Chemother. 1956; 11:379–393. [PubMed: 13383117]
8. Fallahi-Sichani M, Honarnejad S, Heiser LM, Gray JW, Sorger PK. Metrics other than potency reveal systematic variation in responses to cancer drugs. Nat Chem Biol. 2013; 9:708–714. [PubMed: 24013279]
9. Yang W, et al. Genomics of Drug Sensitivity in Cancer (GDSC): a resource for therapeutic biomarker discovery in cancer cells. Nucleic Acids Res. 2013; 41:D955–61. [PubMed: 23180760]
10. Goutelle S, et al. The Hill equation: a review of its capabilities in pharmacological modelling. Fundam Clin Pharmacol. 2008; 22:633–648. [PubMed: 19049668]
11. Tyson DR, Garbett SP, Frick PL, Quaranta V. Fractional proliferation: a method to deconvolve cell population dynamics from single-cell data. Nat Methods. 2012; 9:923–928. [PubMed: 22886092]
12. Frick P, Paudel B, Tyson D, Quaranta V. Quantifying Heterogeneity and Dynamics of Clonal Fitness in Response to Perturbation. J Cell Physiol. 2015; doi: 10.1002/jcp.24888
13. Shoemaker RH. The NCI60 human tumour cell line anticancer drug screen. Nat Rev Cancer. 2006; 6:813–823. [PubMed: 16990858]
14. Quaranta V, et al. Trait variability of cancer cells quantified by high-content automated microscopy of single cells. Meth Enzymol. 2009; 467:23–57. [PubMed: 19897088]
15. Gong Y, et al. Induction of BIM is essential for apoptosis triggered by EGFR kinase inhibitors in mutant EGFR-dependent lung adenocarcinomas. PLoS Med. 2007; 4:e294. [PubMed: 17927446]
16. Seashore-Ludlow B, et al. Harnessing Connectivity in a Large-Scale Small-Molecule Sensitivity Dataset. Cancer Discovery. 2015; 5:1210–1223. [PubMed: 26482930]
17. Rees MG, et al. Correlating chemical sensitivity and basal gene expression reveals mechanism of action. Nat Chem Biol. 2016; 12:109–116. [PubMed: 26656090]
18. McDermott U, Sharma SV, Settleman J. High-throughput lung cancer cell line screening for genotype-correlated sensitivity to an EGFR kinase inhibitor. Meth Enzymol. 2008; 438:331–341. [PubMed: 18413259]
19. Heiser LM, et al. Integrated analysis of breast cancer cell lines reveals unique signaling pathways. Genome Biol. 2009; 10:R31. [PubMed: 19317917]
20. Sporn MB, Harris ED. Proliferative diseases. Am J Med. 1981; 70:1231–1235. [PubMed: 6263092]
21. Seber, GAF.; Wild, CJ. Nonlinear Regression. John Wiley & Sons, Inc; 2005.
22. Ritz C, Streibig JC. Bioassay analysis using R. Journal of Statistical Software. 2005
23. Cornish-Bowden, A. Fundamentals of Enzyme Kinetics. Wiley-Blackwell; 2012.
24. Rein M. The Partial-Equilibrium Approximation in Reacting Flows. Physics of Fluids A - Fluid Dynamics. 1992; 4:873–886.

25. Soetaert K, Petzoldt T, Setzer RW. Solving Differential Equations in R: Package deSolve. Journal of Statistical Software. 33:1–25. [PubMed: 20808728]

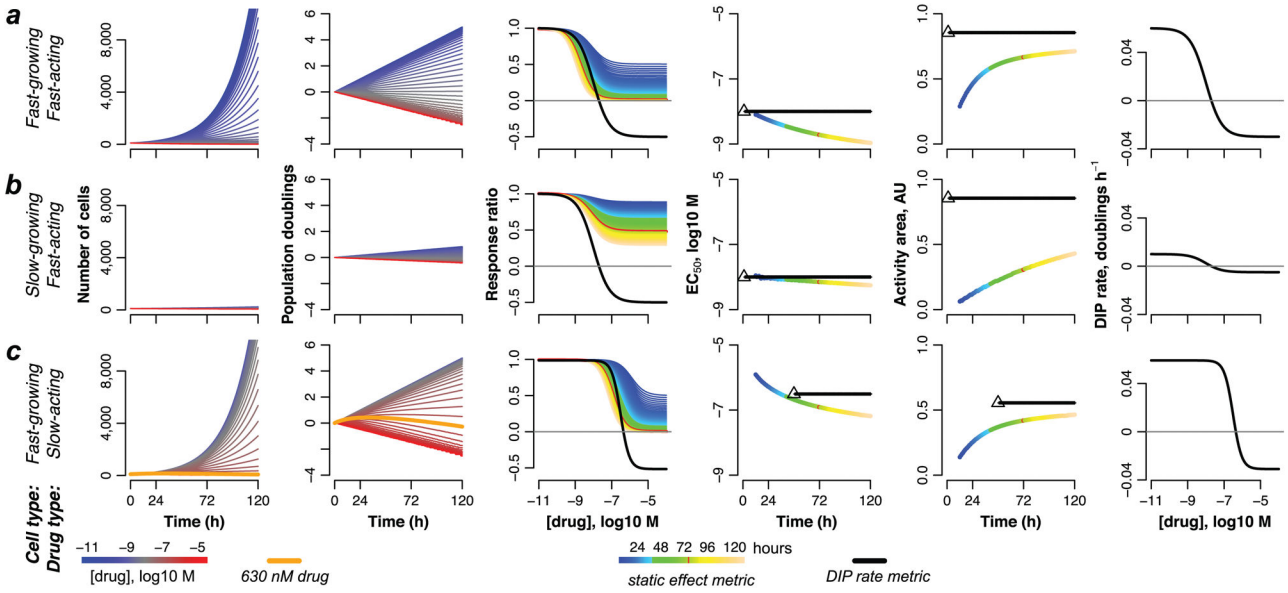

Figure 1. Theoretical illustration of bias in dose–response curves based on static metrics of drug effect

Computational simulations of the effects of drugs on: **(a)** a fast-growing cell line treated with a fast-acting drug; **(b)** a slow-growing cell line treated with a fast-acting drug; **(c)** a fast-growing cell line treated with a slow-acting drug. In all cases, *in silico* growth curves, plotted in linear (*column 1*) and $\log_2$ (*column 2*) scale, are used to generate static- (*column 3*) and DIP rate-based (*columns 3 and 6*) dose–response curves, from which values of EC_{50} (*column 4*) and activity area (AA; *column 5*) are extracted. For DIP rate-based values of EC_{50} and AA, the black triangle denotes the first time point used to calculate the DIP rate (i.e., after the drug effect has stabilized; see Online Methods); the black dashed line signifies that the value remains constant for all subsequent time points. Note that the "response ratio" (*column 3*) and "direct effect" (*column 6*) versions of the DIP rate-based dose–response curves (Supplementary Fig. 1) convey complementary information about the activity of a drug on a cell line (see Supplementary Note for further discussion).

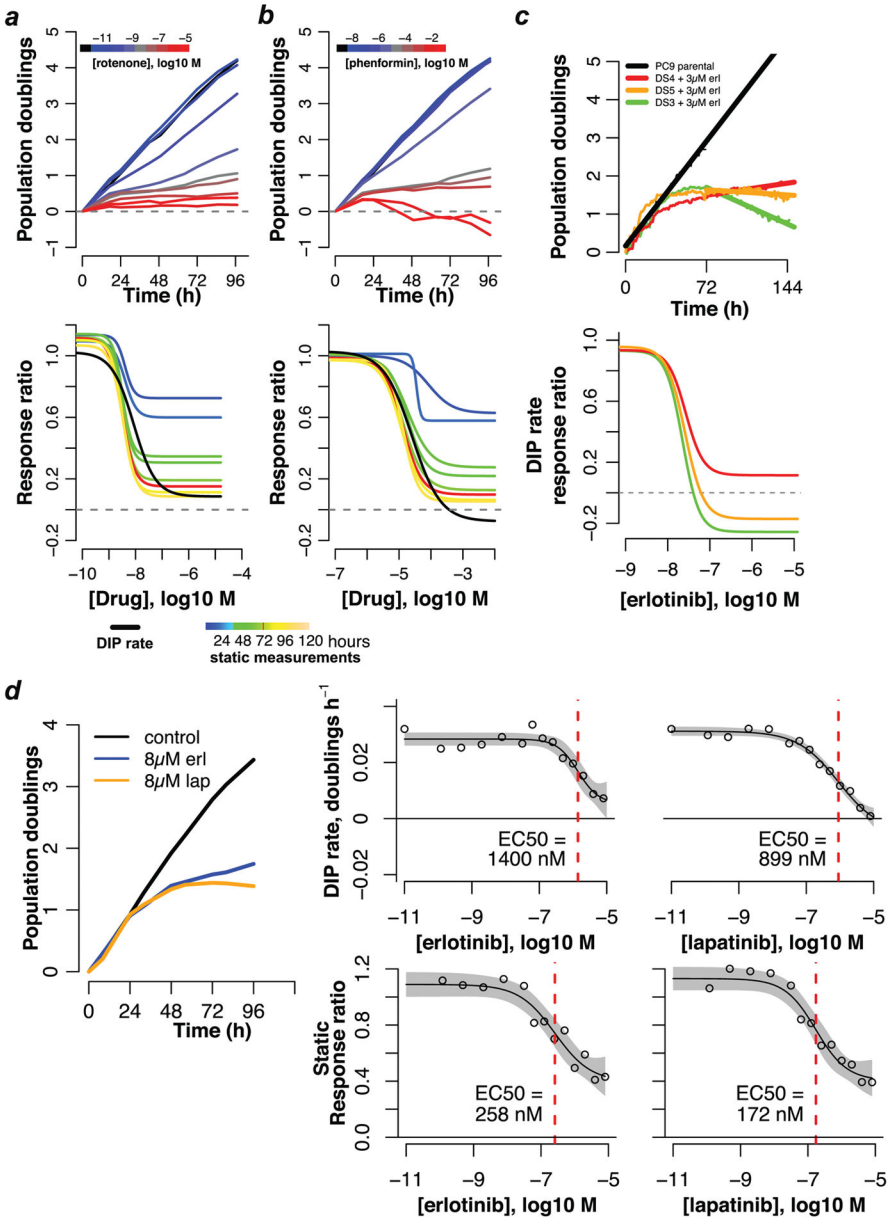

Figure 2. Experimental illustration of time-dependent bias in dose–response curves for drug-treated cancer cells

Population growth curves ($\log_2$ scaled) and derived dose–response curves (static- and/or DIP rate-based) for **(a)** MDA-MB-231 triple-negative breast cancer cells treated with rotenone; **(b)** MDA-MB-231 cells treated with phenformin; **(c)** three single-cell-derived drug-sensitive (DS) clones of the EGFR mutant-expressing lung cancer cell line PC9 treated with erlotinib; **(d)** HCC1954 HER2-positive breast cancer cells treated with erlotinib and lapatinib. Data for (*a*) and (*b*) are from single experiments with technical duplicates; data in (*c*) are from individual wells for two experiments containing technical duplicates (growth curves) and from a single experiment with technical duplicates (dose–response curves); data in (*d*) are sums of technical duplicates from a single experiment (growth curves) and mean values

(circles) with 95% confidence intervals (gray shading) on the log-logistic model fit (dose–response curves; n=4, 6 for erlotinib and lapatinib, respectively).

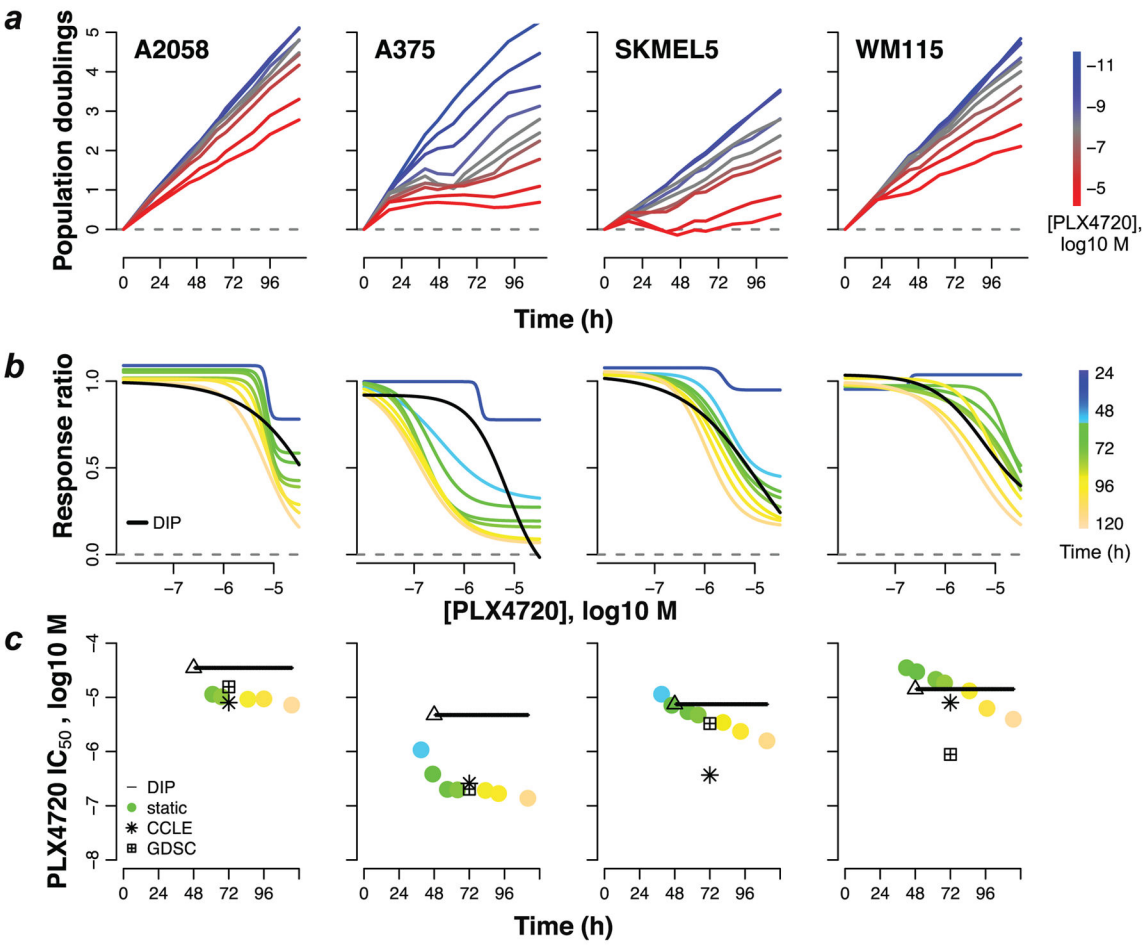

Figure 3. Bias in potency metrics from publicly available data sets

(a) Population growth curves ($\log_2$ scaled) for four select BRAF-mutant melanoma cell lines treated with various concentrations of the BRAF inhibitor PLX4720; **(b)** dose–response curves based on the static effect metric (colored lines) and DIP rate (black line); (**c**) static- (circles) and DIP rate-based (triangle+line) estimates of IC_{50} for each measurement time point. IC_{50} values obtained from public data sets (CCLE: Cancer Cell Line Encyclopedia; GDSC: Genomics of Drug Sensitivity in Cancer), based on the static 72h drug effect metric, are included for comparison. The triangle denotes the first time point used in calculating the DIP rate and the black line signifies that the value remains constant for all subsequent time points. Data shown are from a single experiment with technical duplicates. Experiment has been repeated at least twice with similar results.